Progress In Electromagnetics Research C, Vol. 50, 113–120, 2014

A Tunable Electromagnetic Bandgap Structure Using Plasma

Asma Kallel*, Jerome Sokoloff, Thierry Callegari, and Olivier Pigaglio

Abstract—A tunable electromagnetic-bangap (EBG) structure based on a double layer slotline using plasma is proposed. The plasma permittivity can be tuned by the electron density. The idea of integrating periodical plasma elements inside the slot to tune the stopband is investigated. An electron density and an electron collision frequency equal to $1.75\,10^{13}\,\mathrm{cm}^{-3}$ and $10^{10}\,\mathrm{s}^{-1}$ respectively, are the plasma parameters selected in this study. The simulations reveal a shift rate of the second stopband equal to 6%. A new configuration of the structure is also proposed to adapt it better to the experimental requirements. Based on the simulation results, adding the plasma elements to the modified configuration shifts the stopband 4% and reduces its bandwidth by 43% (at $-20\,\mathrm{dB}$).

1. INTRODUCTION

The electromagnetic bandgap (EBG) structures, also known as photonic crystals, are periodical lattices of metallic or dielectric elements [1]. The electromagnetic waves are reflected by such structures in a frequency band that depends on the lattice characteristics. The tunability of EBG materials is a topical issue, since recent works propose several technologies to control the bandgap, to avoid redesigning the dimensions when the operating frequency changes. In particular, in [2, 3] for example, de Lustrac et al. used PIN diodes to control a conductance lattice. Karim et al. proposed in [4] a tunable bandstop filter by adding MEMS to an EBG material. Also, in [5], Poilasne et al. joined field effect transistors with a metallic EBG material to control the shape of the beam radiated by an antenna. In addition to these devices, some materials can be used for their intrinsic reconfigurability. Indeed, John and Busch obtained in [6] a tunable bandgap of a photonic crystal by adding a liquid crystal. In [7], Yun and Chang used a piezoelectric transducer to control an EBG material. Also, a tunable EBG array was obtained by Kuylenstierna et al. in [8] by using ferroelectric films.

In our study, we propose the use of plasma as an original technology of reconfigurability for tunable EBG structures. Previous works investigated the use of this gas to control the EBG materials. In particular, Sakai et al. [9] created an EBG structure based on discharges arrays. This approach is faced mainly with the issue of plasma losses and the need for high amounts of power to create the plasma elements. To overcome these problems, Giroud et al. [10], Lo et al. [11] and Varault et al. [12, 13] proposed to place single plasma elements as defects in EBG lattices. In these works, the main issue was the difficulty of integrating the plasma electrodes in the original structure.

The objective of this paper is to find configurations that allow to integrate the plasma by easy ways, in contrast with the previous works. We treat here only the microwave dimensioning, as we have proceeded for the 2-D EBG structure in [10]. We propose in this work two configurations of a 1-D EBG structure inspired from [14], and we investigate the idea of adding periodical plasma elements to the structure in order to tune the stopband by adjusting its position and its bandwidth. Moreover, in our study the dielectric losses of the plasma are low.

The paper is organized as follows. In Section 2, we present the EBG structure used in our work. Section 3 describes the tunability property of plasmas by integrating periodical discharges in

Received 13 March 2014, Accepted 16 May 2014, Scheduled 22 May 2014

* Corresponding author: Asma Kallel (asma.kallel@laplace.univ-tlse.fr).

The authors are with the LAPLACE (Laboratoire Plasma et Conversion d'Energie), UPS, INPT, Université de Toulouse, 118 Route de Narbonne, F-31062 Toulouse Cedex 9, France.

the original structure. Also we choose in the same section the plasma parameters taking into account the experimental constraints. In Section 4, we propose a modified configuration of the structure that is more adapted to the experimental conditions of our laboratory. The design of an excitation source adapted to be put in a bell jar with the EBG prototype is also described in this section. Finally, Section 5 concludes the paper.

2. SLOTLINE EBG STRUCTURE

Our study is based on the EBG structure proposed by Boisbouvier et al. [14]. Two dielectric layers of relative permittivity $\varepsilon_r = 3.55$ and loss tangent $\delta = 2.7\,10^{-3}$ are placed on both sides of a slotline constituted of two metallic sheets. The thickness of the substrates t is 0.813 mm and the width W and height h of the slot are 0.5 mm and 0.185 mm, respectively. Periodical metallic discs whose diameter is $d = 6$ mm are etched on either side, as illustrated in Figure 1. The period a is equal to 18.4 mm. The bandgap of such device is periodical and can be predicted as

$$f_m = \frac{m}{2a\sqrt{\varepsilon_{eff}\mu_0}}, \tag{1}$$

where ε_{eff} is the effective permittivity of the hole structure and m is a positive integer. The structure has been simulated using a commercial full-wave solver HFSS [15]. Figure 2(a) depicts the simulated dispersion diagram for the two first stopbands (corresponding to $m = 1$ and 2 in (1)) with the central frequencies of 5.1 GHz and 10.15 GHz, respectively. The simulated transmission coefficient in the case of a device with 5 pairs of discs is shown in Figure 2(b). Only the S_{21} is presented in this figure for clarity. The observed stopbands are consistent with the dispersion diagram. However, we point out the presence of spurious resonances at the out-of-stopband regions. This problem can be addressed by introducing low-pass structures within the device, as suggested by [16].

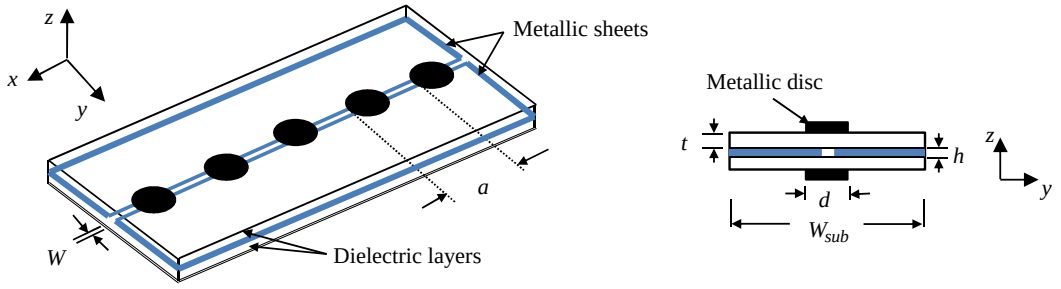

Figure 1. Geometry of the slotline EBG structure. The left-hand figure is a 3D view and the right-hand one is a transversal view. $a = 18.4$ mm, $W = 0.5$ mm, $h = 0.185$ mm, $d = 6$ mm and $t = 0.813$ mm.

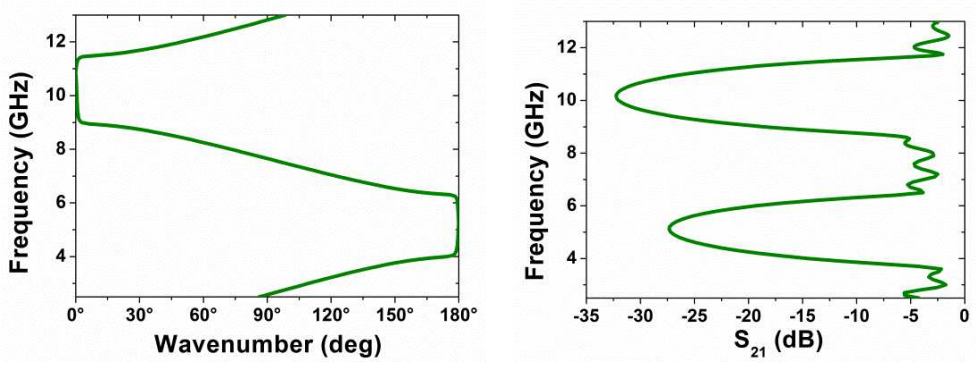

Figure 2. (a) Simulated dispersion diagram of the EBG structure. (b) Simulated transmission coefficient of the 5 period EBG structure.

3. TUNABLE SLOTLINE EBG STRUCTURE

3.1. Plasma Integration

In this study, we assume that the plasma relative permittivity follows the Drude model given by

$$\varepsilon_p = \varepsilon'_p - j\varepsilon''_p = 1 - \omega_p^2/\left(\omega^2 - j\omega\nu\right), \tag{2}$$

where ν is the electron collision frequency and ω_p is the plasma angular frequency. The electron density is given by $n_e = \varepsilon_0 m_e \omega_p^2/e^2$, where m_e and e are the electron mass and charge respectively. In practice, n_e can be controlled by the voltage applied between the electrodes. ν, however, is mainly related to the gas pressure and induces electromagnetic losses in plasma. The input parameters (n_e, ν) then control the complex permittivity of plasma so that $-\infty < \varepsilon'_p \leq 1$. Hence, this interesting property can be used to make the proposed device reconfigurable. Moreover, the proposed EBG configuration provides a possibility to integrate the plasma without disrupting the functioning. Indeed, the presence of an empty slot in the EBG structure allows the creation of a plasma inside it.

We begin our analysis by investigating the idea of creating an EBG based solely on a plasma array. We simulate a configuration where the discs are removed and 5 periodical plasmas are created inside the slot. Figure 3(a) depicts the longitudinal section of this configuration along the slot. Figure 3(b) shows the transmission coefficient S_{21} obtained with the full-wave solver for two types of plasmas. In the case of the lossless plasma ($n_e = 10^{13}\,\mathrm{cm}^{-3}$, $\nu = 0$), a stopband appears around 6.50 GHz. When we take into account the electron collisions to model a lossy plasma ($n_e = 3\,10^{13}\,\mathrm{cm}^{-3}$, $\nu = 10^{10}\,\mathrm{s}^{-1}$), the bandgap is tuned as expected but is concealed by the plasma losses. These results are consistent with the issue of plasma losses in the EBG arrays of Sakai et al. [9]. For this reason, we have chosen to keep the original structure with the metallic discs as illustrated in Figure 1 instead of periodical plasmas. On the one hand, the presence of the discs aims at creating the stopband, and on the other hand, adding the plasma aims at tuning the central frequency. This configuration is worthwhile since each pair of discs facing each other can play the role of electrodes to create the plasma. Hence, no electrode has to be added to the structure, which avoids the disruption of its functioning.

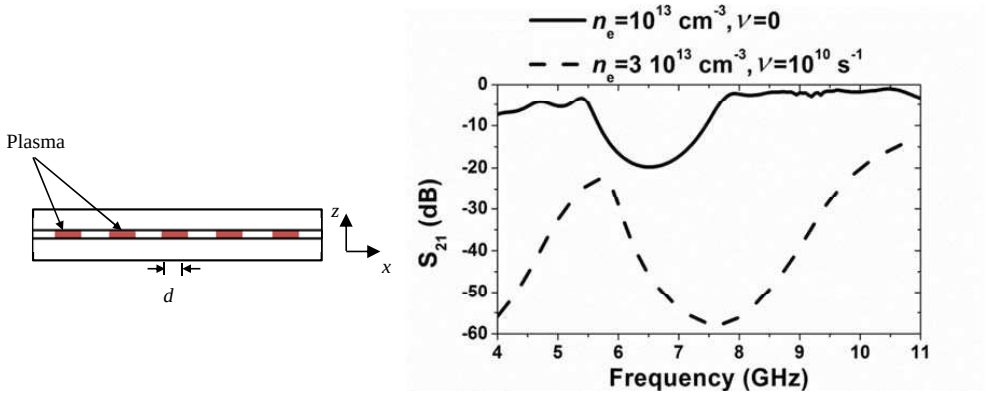

Figure 3. (a) Longitudinal section along the slot of the bilayer slotline without discs. Red regions represent periodical plasma elements in the slot. (b) Simulated bandgap feature in the case of the configuration shown in (a) for 2 different plasma parameters (see legend).

3.2. Choice of the Plasma Parameters

In order to limit the effect of the plasma losses on the transmission in the out-of-stopband region, we choose to focus our study on the second bandgap (see Figure 2), since ε''_p decreases with the frequency. We start our analysis by integrating 5 lossless plasmas at $n_e = 10^{13}\,\mathrm{cm}^{-3}$, each one located between a pair of discs facing each other, as illustrated in Figure 4(a). It is observed from the transmission coefficients of

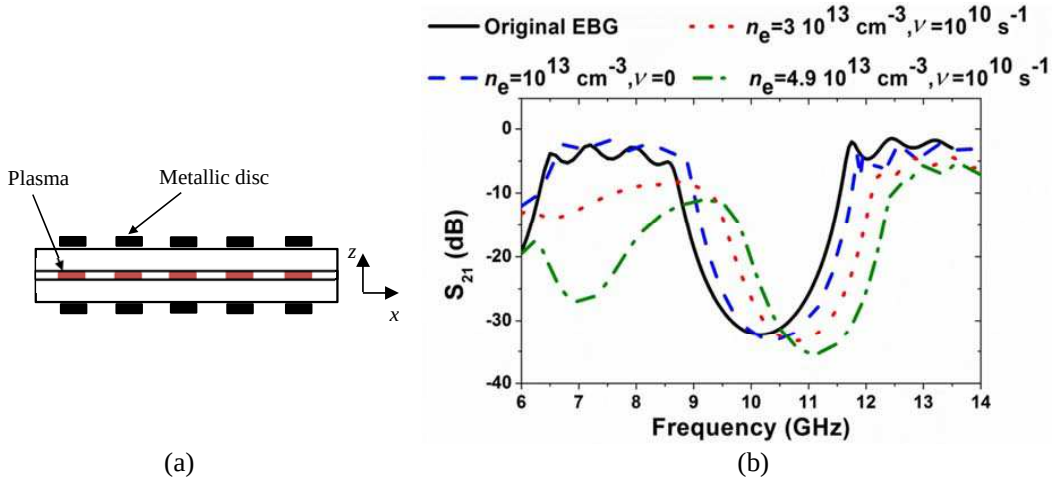

Figure 4. (a) Longitudinal section along the slot of the EBG structure with 5 periodical plasma elements (shown in red). (b) A comparison of the simulated bandgap position for different parameters of plasma with regard to the original EBG structure (see legend).

Figure 4(b) that the presence of the plasma elements involves a shift in the second stopband. In practice, we are not able to create such a plasma as electron collisions are unavoidable. Indeed, Figure 4(b) shows two examples of lossy plasmas ($n_e = 3\,10^{13}\,\mathrm{cm}^{-3}$, $\nu = 10^{10}\,\mathrm{s}^{-1}$) and ($n_e = 4.9\,10^{13}\,\mathrm{cm}^{-3}$, $\nu = 10^{10}\,\mathrm{s}^{-1}$). We note here that the stopband moves to the higher frequencies with the electron density. This demonstrates the reconfigurability of the EBG structure by means of plasma. We observe also a degrading of the transmission in these cases due to the presence of electron collisions.

Actually, the stopband position is controlled by the real part of the relative permittivity ε'_p. The higher $|\varepsilon'_p|$ is the more important the stopband shift is. ε'_p is mainly controlled by n_e (its absolute value increases with n_e). However, based on (2), the frequency of electron collisions also affects the value of ε'_p. As a consequence, the shift rate produced by a lossless plasma, for instance, is different from the one produced by a plasma having the same density and with collisions.

Based on the last remark,we aim in this section at choosing the parameters of the lossy plasma that, on the one hand, shift the stopband with a rate comparable to that obtained with the lossless plasma of Figure 4(b) and on the other hand reduce the intrinsic losses. This amounts to finding the parameters (n_e, ν) that make the corresponding ε_p fit the permittivity of the lossless plasma in the frequency range $I = [8\text{–}13\,\mathrm{GHz}]$. In our problem, we impose the constraints $n_e \in C_1$ and $\nu \in C_2$, where $C_1 = [10^{10} - 10^{14}\,\mathrm{cm}^{-3}]$ and $C_2 = [10^{10} - 10^{12}\,\mathrm{s}^{-1}]$. C_1 and C_2 are respectively the density and the frequency of electron collisions ranges that we have chosen based on experimental considerations. Our numerical algorithm finds the solution $S = (n_e = 1.75\,10^{13}\,\mathrm{cm}^{-3}, \nu = 10^{10}\,\mathrm{s}^{-1})$ which represents the parameters of the selected plasma.

Figure 5 depicts the dispersion diagram and the transmission coefficient of the EBG structure and periodical plasmas with the selected parameters. Compared to the original structure, the central frequency of the stopband is moved to 10.75 GHz, i.e., the stopband shift rate is $\Delta f/f = 6\%$, which is a good rate compared with the performances of the technologies cited in the introduction.

Figure 6 depicts the proposed supply for the creation of the plasma in this configuration. In order to create localized periodical plasmas, either pair of discs facing each other acts as electrodes. The presence of the dielectric layers imposes the use of an AC supply, as shown in Figure 6(a). In this case, the plasma is on only for a short time of about 100 µs. To overcome this problem, a DC voltage is then applied between the metallic sheets of the slotline, as illustrated in Figure 6(b).

The main issue in this configuration is the dimensions of the plasmas we should create. Indeed, based on our experience feedback, it is difficult to reach the desired density and collision frequency at the same time in such a small volume, given the slot dimensions. A new configuration is then proposed in the next section.

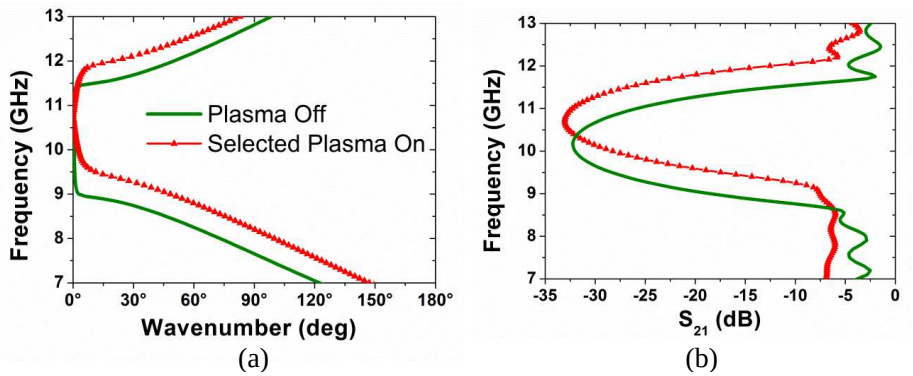

Figure 5. (a) Comparison of the simulated dispersion diagrams of the original structure and with 5 periodical selected plasmas. (b) Comparison of the simulated S_{21} in the same cases of (a).

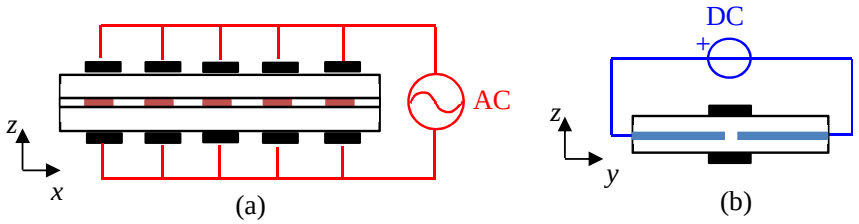

Figure 6. (a) A longitudinal section showing the principle of the AC supply. (b) A transversal view of the structure showing the principle of the DC supply.

4. DESIGN OF A NEW CONFIGURATION OF THE SLOTLINE STRUCTURE

4.1. Addition of Holes

To overcome the issue of the plasma volume, we increase the height of this region by making holes in the substrate on both sides of the slot, as depicted in Figure 7(a). However, increasing the plasma volume in that way induces more losses in the out-of-stopband region. To get around this problem, we lower the plasma length l in the x direction. Parametric simulations lead us to the choice of a length of 3 mm since it reduces the impact of intrinsic losses and at the same time keeps approximately the same tunability ability. The longitudinal section of the new structure in Figure 7(b) shows the 10 holes made in the substrates. Figure 8 reveals the simulated S-parameters of this configuration. It is observed that the central frequency of the stopband is slightly moved to 10.20 GHz with regard to the original structure (without holes). Filling the 5 appropriate regions with the selected plasma produces a shift of the stopband of 10.60 GHz, i.e., $\Delta f/f = 4\%$. The fall in the bandgap shift is explained by the reduction

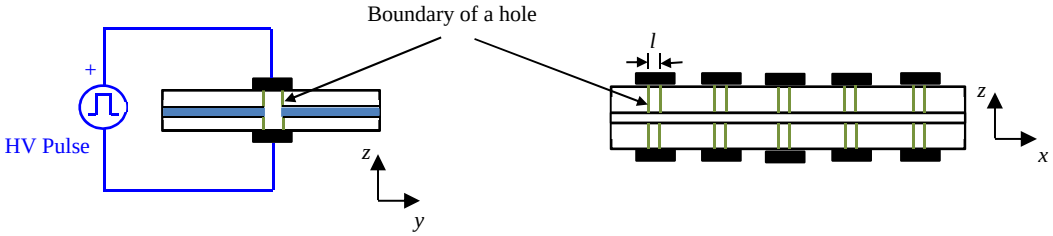

Figure 7. (a) A transversal section along a disc axis showing the holes (boundaries in green lines) made in the 2 dielectric layers. The principle of the high voltage pulse supply is shown in blue lines. (b) The longitudinal section along the slot. The length of each hole in the x direction.

of the plasma length in the x direction. However, it should also be noted that, in the new configuration, adding the plasma tunes also the bandgap bandwidth. Indeed, the bandwidth is reduced by about 43% (at -20 dB) when the plasmas are turned on. Furthermore, the simulated prototype is not optimized which has led to a low level of S_{21} in the passband regions. This issue is not treated here since the main objective in this paper is to validate the concept of tuning the stopband.

In this configuration, as the dielectric has been removed at the holes, we propose the use of only one high voltage pulse power supply connected to each pair of discs facing each other to create localized plasmas, as depicted in Figure 7(a).

4.2. Design of the Excitation Source

Our final prototype will be put in a bell jar, shown in Figure 9, in our laboratory in order to control the pressure of the plasma. This imposes maximum dimensions of the prototype that should not be exceeded. Hence, we propose the use of a microstrip line as an excitation source since its dimensions are adapted to be inserted into the bell jar with the EBG structure. As depicted in Figure 10, a microstrip-to-slotline multisection transition is dimensioned based on the configuration proposed by Tu and Chang [17]. The dimensions of the transitions are listed in Table 1. It is worthy to note that the thickness of the metallic sheets h is assumed to be equal to 0.235 mm in the design, which does not alter our results.

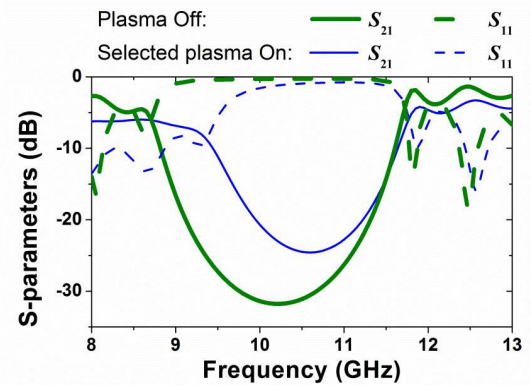

Figure 8. Comparison of the simulated S-parameters of the new configuration when plasma is off and when 5 selected plasmas are on (see legend).

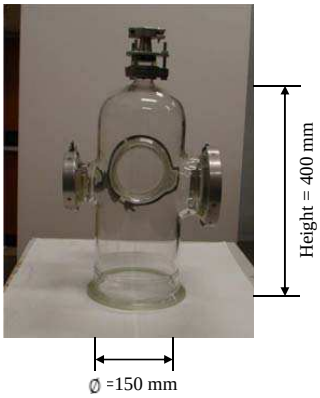

Figure 9. A photography of the bell jar to be used for measurements in our laboratory. Its height is 400 mm and its diameter is 150 mm.

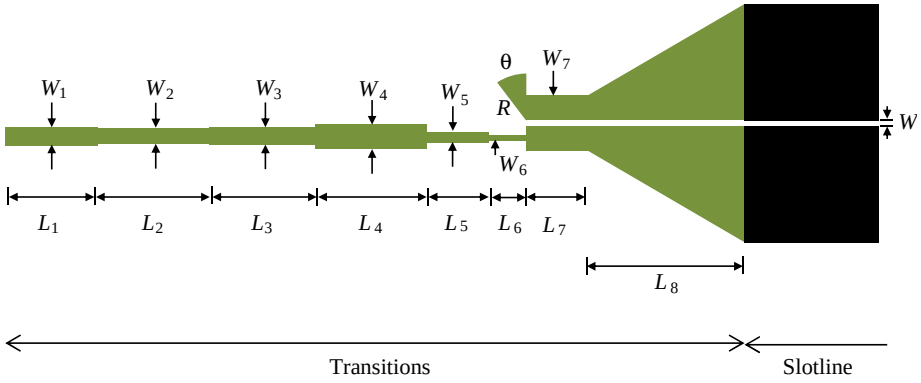

Figure 10. Configuration of the microstrip-to-slotline multisection transition. The green lines are the transitions and the dark line is the slotline.

Table 1. Dimensions of the transitions.

Transition	W_1/L_1	W_2/L_2	W_3/L_3	W_4/L_4	W_5/L_5	W_6/L_6	W_7/L_7	R/θ	L_8
Dimension (mm)	1.95/8.5	1.7/8.9	1.8/9.6	2.2/9	1.1/5.6	0.3/3	2/3.2	3.8/50°	9

5. CONCLUSION

In this paper, we have proposed a tunable EBG slotline using plasma. We have shown the ability of plasma discharges to move the stopband, since the electron density, and thereby the permittivity, can be controlled by the voltage applied between the electrodes. This structure provides the possibility of plasma creation without adding electrodes. An electron density and an electron collision frequency ($n_e = 1.75\,10^{13}\,\mathrm{cm}^{-3}$, $\nu = 10^{10}\,\mathrm{s}^{-1}$) have been chosen in ranges based on experimental considerations. Full-wave simulations show that the selected plasma produces a shift rate of 6%. In order to make the desired discharge easier to create, we have modified the EBG structure by adding holes in the substrates. The new configuration allows the tuning of the bandgap position and of its bandwidth. The simulations of the new configuration reveal a shift rate of 4% and a reduction of the bandwidth of 43%. Moreover, in order to adapt our prototype dimensions to the bell jar in where it will be put for plasma creation, we have chosen a microstrip line as an excitation source and we have designed transitions that guarantee the matching to the EBG structure. One of the applications of the proposed device is a tunable band-stop filter.

A study of the feasibility of the selected plasma parameters in the second configuration is in progress using a numerical model, before moving to the experimental tests.

REFERENCES

1. Notomi, M., "Theory of light propagation in strongly modulated photonic crystals: Refractionlike behaviour in the vicinity of the photonic band gap," *Physical Review B*, Vol. 62, 10696–10705, 2000.
2. De Lustrac, A., F. Gadot, E. Akmansoy, and T. Brillat, "High-directivity planar antenna using controllable photonic bandgap material at microwave frequencies," *Applied Physics Letters*, Vol. 78, 4196–4198, 2001.
3. De Lustrac, A., F. Gadot, S. Cabaret, J. M. Lourtioz, A. Priou, E. Akmansoy, and T. Brillat, "Experimental demonstration of electrically controllable photonic crystals at centimeter wavelengths," *Applied Physics Letters*, Vol. 75, 1625–1627, 1999.
4. Karim, M. F., A. Q. Liu, A. B. Yu, and A. Alphones, "MEMS-based tunable bandstop filter using electromagnetic bandgap (EBG) structures," *APMC 2005, Asia-Pacific Microwave Conference Proceedings*, Vol. 3, 4–7, Dec. 2005.
5. Poilasne, G., P. Pouliguen, K. Mahdjoubi, L. Desclos, and C. Terret, "Active metallic photonic band-gap materials (MPBG): Experimental results on beam shaper," *IEEE Transactions on Antennas and Propagation*, Vol. 48, No. 1, 117–119, 2000.
6. John, S. and K. Busch, "Liquid-crystal photonic-band-gap materials: The tunable electromagnetic vacuum," *Physical Review Letters*, Vol. 83, No. 5, 967–970, 1999.
7. Yun, T.-Y. and K. Chang, "An electronically tunable photonic bandgap resonator controlled by piezoelectric transducer," *IEEE MTT-S International Microwave Symposium Digest*, Vol. 3, 1445–1447, Jun. 2000.
8. Kuylenstierna, D., A. Vorobiev, G. Subramanyam, and S. Gevorgian, "Tunable electromagnetic bandgap structures based on ferroelectric films," *IEEE Antennas and Propagation Society International Symposium*, Vol. 4, 879–882, 2003.
9. Sakai, O., T. Sakaguchi, and K. Tachibana, "Plasma photonic crystals in two-dimensional arrays of microplasmas," *Contrib. Plasma Phys.*, Vol. 47, 96, 2007.
10. Giroud, L., J. Sokoloff, and O. Pigaglio, "Reconfigurable EBG at 18 GHz using perimeter defects," *Journal of Electromagnetic Waves and Applications*, Vol. 23, Nos. 8–9, 1029–1037, 2009.

11. Lo, J., J. Sokoloff, T. Callegari, and J. P. Boeuf, "Reconfigurable electromagnetic band gap device using plasma as a localized tunable defect," *Applied Physics Letters*, Vol. 96, No. 25, 251501, 2010.
12. Varault, S., B. Gabard, J. Sokoloff, and S. Bolioli, "Plasma-based localized defect for switchable coupling applications," *Applied Physics Letters*, Vol. 98, No. 13, 134103, 2011.
13. Varault, S., B. Gabard, T. Crépin, J. Sokoloff, and S. Bolioli, "Reconfigurable modified surface layers using plasma capillaries around the neutral inclusion regime," *J. Appl. Phys.*, Vol. 115, 084906, 2014.
14. Boisbouvier, N., A. Louzir, F. Le Bolzer, A. C. Tarot, and K. Mahdjoubi, "A double layer EBG structure for slot-line printed devices," *IEEE Antenna and Propagation Society International Symposium*, Vol. 4, 3553–3556, 2004.
15. Ansoft Corporation, Online Available: http://www.ansoft.com.
16. Quendo, C., E. Rius, C. Person, and M. Ney, "Integration of optimized low-pass filters in a bandpass filter for out-of-band improvement," *IEEE Transactions on Microwave Theory and Techniques*, Vol. 49, No. 12, 2376–2383, 2001.
17. Tu, W.-H. and K. Chang, "Wide-band microstrip-to-coplanar stripline/slotline transitions," *IEEE Transactions on Microwave Theory and Techniques*, Vol. 54, No. 3, 1084–1089, 2006.